Rapid DCE-MRI parameter generation using principal component analysis and clustering

Martin Lowry[1], Lawrence Kenning[2], and Lindsay W Turnbull[1]

[1]*Centre for MR Investigations, Hull York Medical School at University of Hull, Hull, East Yorkshire, United Kingdom,* [2]*Centre for MR Investigations, University of Hull, Hull, East Yorkshire, United Kingdom*

Introduction: Dynamic contrast-enhanced MRI (DCE-MRI) has considerably potential to evaluate tumour status at presentation, during treatment and for interval follow-up[1] through its ability to assess the state of the blood-brain barrier and blood vessel patency in gliomas. It is likely to gain in importance with the advent of new vascular-targeted therapies for high-grade lesions. Absolute quantification of the data, however, is hampered, first, by the technical demands of the acquisition – rapid sampling and heavy T_1 weighting – which generate low SNR images. Secondly, spatial heterogeneity of the derived parameters necessitates a voxel-based, rather than region-based, estimation of their values and thus increases the computational demand. Here we report a method that simultaneously reduces the impact of both these limitations to rapidly produce parameter maps with increased precision. This method may be of interest to clinicians, and both clinical and basic scientists.

Methods: DCE-MRI was performed as part of a multi-parametric examination in 80 patients with histologically proven gliomas of various grades. They were scanned using a 3.0T system (GE MR750 Discovery) and an eight channel phased array head coil. Morphological imaging in the form of T_2 FLAIR and T_1 contrast imaging was acquired along with diffusion tensor imaging, spectroscopy, DCE and dynamic susceptibility-weighted imaging. The DCE-MRI was acquired with a 3D FSPGR sequence using a TR/TE of 5.0/1.6ms, flip angle of 20°, FOV of 24 x 19.2 x 8cm, matrix of 192 x 96 x 20 and 2-fold parallel imaging acceleration. Sixty phases where acquired at a temporal resolution of 5s. Contrast (0.5M Gadoteric acid; dose, 0.075mmol/kg body wt) was administered by pump after the fourth phase at 4ml/s. Native tissue T_1 was measured using a series of 5 multi-flip angle T_1 volumes (3°, 5°, 10°, 20°, 40° flip angles) prior to the DCE-MRI.

In preliminary processing motion within the dynamic series and between this and the multi-flip angle sequences was minimised by applying a series of motion correcting registrations using FSL[2]. All data was subsequently processed using in-house software developed in IDL. Signal intensity time courses for all voxels within the brain on each slice showing a positive IAUC were converted to contrast concentration time courses using T_1 values calculated from the multi-flip angle data. To improve the speed and precision of processing we then subjected these curves to a two-stage data reduction process. First, principal component analysis (PCA) was performed to allow removal of noise in the data. As many components as were required to recover 98% of the data variance were retained and used to divide the curves into a maximum of 160 clusters using the *k*-means algorithm. Reduced noise curves were reconstructed from the same minimal principal component set and the median curve of each cluster used for pharmacokinetic (PK) analysis. PK modelling used a two compartment extended Tofts-Kety model with a population AIF[3]. PK parameter values estimated from each median curve were assigned to all member voxels of the cluster to produce parameter maps.

Results: We illustrate our method with one example case from our series of patients, however similar performance was observed in all cases. This patient had an extensive deep seated high-grade lesion unsuitable for resection and survived only 126 days after presentation. Typical SNR values of the pre-contrast images in a central slice of the volume were 20-40. The 15 useable slices produced 102,821 voxels which passed the quality criteria and which, using a single thread on a 2.8GHz i7 processor took 52 minutes to process at ~30ms/voxel. Using our method with PCA and clustering we were able to reproduce essentially identical PK parameter maps in less than 1 minute (fig. 1). Further improvements were possible through parallel processing on multiple processors. Note particularly the absence of spurious high-valued voxels in the V_e map and the more complete V_b map when using our method. This improvement is primarily due to a reduction in the number of passes through the fitting routine, since although the number of voxels was reduced to 1,420 clusters (mean: 95/slice) the fitting of each cluster's median curve took about 42ms to converge, probably reflecting the reduced noise in each curve(fig 2). The bottleneck now becomes the clustering algorithm rather than the least squares fitting. Mean values for K^{trans}, V_e and V_b for an ROI encompassing the whole of the lesion for the illustrated slice were respectively 0.27 ± 0.12 vs. 0.25 ± 0.11min^{-1}, 0.63 ± 0.19 vs. 0.60 ± 0.17 and 0.04 ± 0.03 vs. 0.06 ± 0.02 and were not significantly different for ±PCA. The use of *k*-means clustering leads to some inherent minor limitations in our technique. First, the random initial cluster assignments preclude an exact reproduction for repeated analyses. Secondly, the parameter values are essentially digitised, however, since the number of clusters is large compared to the range of the parameter values this digitisation falls within the error of measurement and thus has little impact on the statistical metrics.

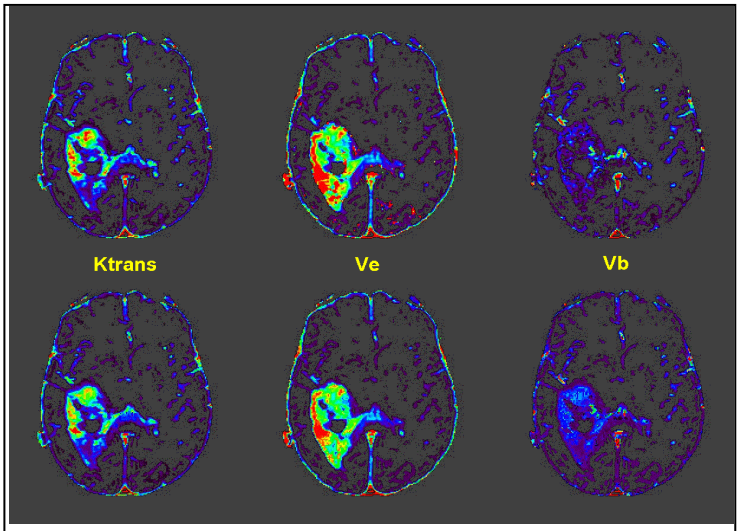

Figure 2. PK parameter maps obtained without (T) and with (B) PCA and clustering.

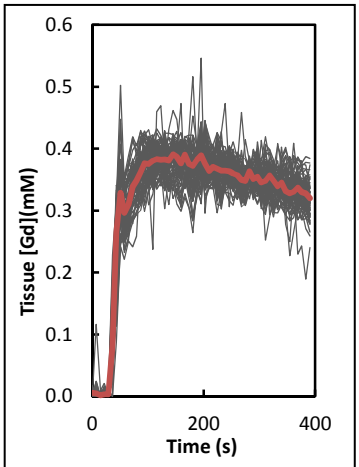

Figure 1. Contrast concentration time course for one cluster of 71 voxels overlaid with their median curve (red).

Conclusion: It is now recognised that quantitative multi-modality imaging, including DCE-MRI, can be a valuable adjunct to morphological imaging in the assessment of tumour burden and response to therapy[4]. The processing method described here which enables an improvement in the speed of parametric map generation should remove the necessity for off-line processing and make the technology more readily available to radiologists.

References: 1. Jain R (2013) NMR Biomed. **26:** 1042-1049. **2**. Jenkinson *et al*. Medical Image Analysis. (2001) **5**: 143-156. **3.** Parker G *et al* (2006) MRM **56**: 993-1000. 4. Roy B *et al* (2013) Neuroradiol. **55**: 603-613 and references therein.